EUROPEAN ORGANIZATION FOR NUCLEAR RESEARCH

L3 Note 2593
July 11, 2000

Search for invisible Higgs boson decays in e^+e^- collisions at $\sqrt{s} = 200 - 209$ GeV

L3 Collaboration

Abstract

A search for a non-minimal Higgs boson decaying into undetectable particles is performed using the data collected by the L3 experiment during the year 2000 at centre-of-mass energies ranging from 200 GeV up to 209 GeV with a total integrated luminosity of 69.3 pb^{-1}. The results of this search are combined with those obtained at lower energies. Assuming this non-minimal Higgs boson has the same production cross section than the Standard Model Higgs boson and a branching ratio into invisible particles of 100%, a preliminary lower limit of 100.0 GeV is derived at the 95% confidence level. These results are preliminary.

Submitted to the *XXXth International Conference on High Energy Physics*
July 27 - August 2, 2000, Osaka, Japan

1 Introduction

In some extensions of the Standard Model, the Higgs boson can decay into stable weakly interacting particles, thus yielding invisible final states [1]. For example in the minimal supersymmetric extension of the Standard Model, the Higgs boson can decay into a pair of undetectable neutralinos.

We search for a Higgs boson signal produced through the Higgs-strahlung process: $e^+e^- \to Z^* \to hZ$. The Z boson decays into a fermion pair: $Z \to f\bar{f}$ and the Higgs boson into invisible particles. We study two different topologies: two acoplanar jets plus missing energy, corresponding to the Z boson hadronic decay and two acoplanar charged leptons plus missing energy corresponding to the Z boson leptonic decay into electrons or muons.

This article describes the analysis done to search for the invisible Higgs boson decays in the data collected by the L3 experiment [2] at LEP during the year 2000 at centre-of-mass energies of $\sqrt{s} = 200,\ 202,\ 204,\ 206$ and 209 GeV. The corresponding integrated luminosities are respectively 0.66, 0.58, 21.18, 47.59, and 1.72 pb^{-1}. Searches for the invisible Higgs boson decays at lower centre-of-mass energies have been reported by the LEP experiments [3].

2 Event simulation

For the signal efficiency, study samples of Higgs boson events are generated using PYTHIA [4] for masses between 60 and 110 GeV.

For the background studies the following Monte Carlo programs are used: PYTHIA ($e^+e^- \to q\bar{q}(\gamma),\ e^+e^- \to Z/\gamma^*Z/\gamma^*$ and $e^+e^- \to Ze^+e^-$), KORALW [5] ($e^+e^- \to W^+W^-$), KORALZ [6] ($e^+e^- \to \mu^+\mu^-(\gamma)$, $e^+e^- \to \tau^+\tau^-(\gamma)$), PHOJET [7] ($e^+e^- \to e^+e^-q\bar{q}$), DIAG36 [8] ($e^+e^- \to e^+e^-\ell^+\ell^-$ with $\ell = e,\mu,\tau$), BHWIDE [9] ($e^+e^- \to e^+e^-(\gamma)$), and EXCALIBUR [10] ($e^+e^- \to f\bar{f}'f''\bar{f}'''$).

The L3 detector response is simulated using the GEANT 3.15 program [11], which takes into account the effects of energy loss, multiple scattering and showering in the detector. The GHEISHA program [12] is used to simulate hadronic interactions in the detector.

3 Search in the hadronic channel

In this channel, denoted $hq\bar{q}$, we use a cut based analysis to select events. We optimize two sequential selections separately for the light (below 80 GeV) and heavy (above 80 GeV) invisible Higgs boson mass ranges.

Unless otherwise stated in this section the events are reconstructed into jets by choosing a $y_{\rm cut}$ in the DURHAM algorithm [13] that corresponds to the two-jet topology.

The event preselection is described in section 3.1, the additional cuts applied for the heavy and light Higgs boson selections are described in sections 3.2 and 3.3, respectively. The number of events, expected and observed, after the application of the different hadronic selections are reported in Tables 1, 2.

3.1 Preselection

The selection of hadronic events is done by requiring a high multiplicity of calorimetric clusters, $N_{CL} \geq 15$ and of charged tracks, $N_{TR} \geq 4$. These two selection criteria substantially reduce the background contamination from the two-photon interactions, referred to as $\gamma\gamma \to e^+e^-q\bar{q}$.

In order to reject beam-gas interactions we demand the selected events to have at least an energy of 10 GeV and 5 GeV in the electromagnetic and hadronic calorimeter, respectively.

At centre-of-mass energies above the Z peak, there is a large background of two-fermion events, denoted $q\bar{q}(\gamma)$, with an initial state radiation to the Z peak. In order to reduce this background we apply a quality cut which requires the jets and the missing momentum vector to be distant from the beam pipe in polar angle, the maximum of their cosine must be less than 0.99 in absolute value. We also demand the sine of the angle between the beam axis and the plane containing the dijet system to be larger than 0.05. We require the effective centre-of-mass energy of the e^+e^- reaction (i.e. after a possible radiation of a photon in the initial state) of the selected events to be larger than 55% of the total centre-of-mass energy. These two latter cuts further reject the $q\bar{q}(\gamma)$ background.

In addition, we veto events with large forward energy deposits, $E_{ALR} < 5$ GeV, $E_{V12} < 10$ GeV, where E_{ALR} and E_{V12} are respectively the energy in the in the small angle calorimeter within $4^\circ < \theta < 9^\circ$ and the visible energy in a 12° cone around the beam pipe. This veto supresses the background from the Ze^+e^- and $q\bar{q}(\gamma)$ processes and from the two-photon interactions.

The missing energy requirement is made through a cut on the visible energy which must lie in the range of 35% up to 70% of the centre-of-mass energy.

Figure 1 displays the comparison between the data and the Monte Carlo expectations on the visible mass (i.e. the dijet invariant mass) distributions after the hadronic preselection.

$hq\bar{q}$ analysis	
N_{data}	267
N_{bg}	254.1
$\gamma\gamma \to e^+e^-q\bar{q}$	2.4
$\gamma^*/Z \to q\bar{q}(\gamma)$	34.2
$W^+W^- - e^\pm\nu_e q\bar{q}'$	147.2
$\gamma^*/Z, \gamma^*/Z$	17.6
$e^\pm\nu_e q\bar{q}'$	51.3
Ze^+e^-	1.5

Table 1: The number of observed events, N_{data}, compared to the number of expected events from Standard Model processes, N_{bg}, after the preselection cuts.

3.2 Heavy Higgs boson selection

In order to insure that there is no overlap between the two hadronic final selections, we split the event sample into the heavy and the light Higgs boson selection categories depending on wether the reconstructed Z boson velocity is smaller or larger than 0.4, respectively.

We require the dijet mass to be compatible with a Z boson by restricting it to be larger than 60 GeV and less than 100 GeV.

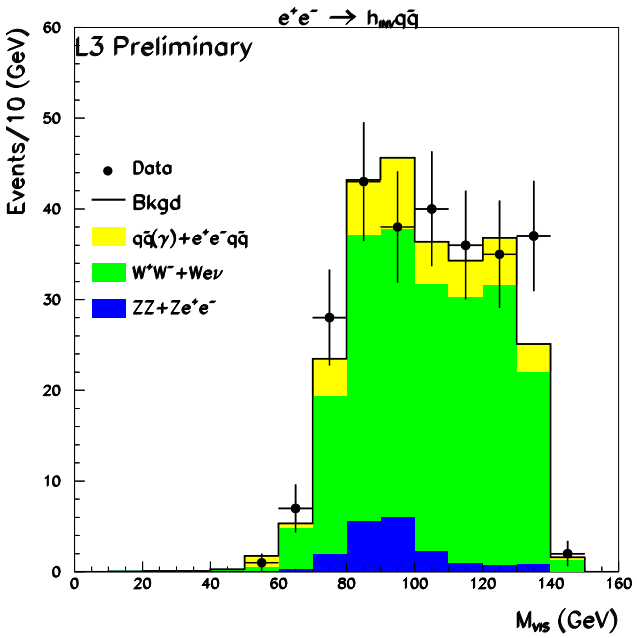

Figure 1: The distribution of the visible mass after the hadronic preselection. The dots represent the data, the solid line histogram represents the total expected background, the black, dark shaded and light shaded areas representing respectively the $Z/\gamma^*Z/\gamma^* + Ze^+e^-$, W^+W^- + $W^{\pm}e^{\mp}\nu_e$ and $q\bar{q}(\gamma) + \gamma\gamma \rightarrow e^+e^-q\bar{q}$ contributions to the total background.

We extend the forward energy veto by requiring the visible energy in a 30° cone around the beam axis to be less than 10 GeV. This supresses the $q\bar{q}(\gamma)$, $\gamma\gamma \rightarrow e^+e^-q\bar{q}$ and Ze^+e^- backgrounds. A further rejection of the $q\bar{q}(\gamma)$ and Ze^+e^- backgrounds is made by demanding the longitudinal momentum imbalance to be less than 30% of the visible energy. The remaining $q\bar{q}(\gamma)$ and Ze^+e^- background contributions are supressed by rejecting events with an acollinearity larger than 126.1°.

We cut on the acoplanarity to lie between 126.1° and 174.8°. This reduces the $q\bar{q}(\gamma)$, $\gamma\gamma \rightarrow e^+e^-q\bar{q}$ and Ze^+e^- background contaminations.

An isolation criterion is applied to the missing momentum vector, such that the energy in a cone of 60° centered on its direction is less than 3 GeV. This requirement reduces the W pair and the single W background contributions.

Tightening the cuts on the visible energy, so that it is between 35% and 55% of the centre-of-mass energy, further supresses the $q\bar{q}(\gamma)$, $\gamma\gamma \rightarrow e^+e^-q\bar{q}$, W^+W^- and Ze^+e^- backgrounds.

We apply a cut on the transverse momentum imbalance, demanding that it is between 20% and 60% of the visible energy. The latter cut removes most of the remaining $q\bar{q}(\gamma)$, $\gamma\gamma \rightarrow e^+e^-q\bar{q}$ and Ze^+e^- background while keeping most of the heavy Higgs boson signal.

Figure 2 displays the comparison between the data and the Monte Carlo expectations on the reconstructed Higgs boson mass distributions after the heavy Higgs boson selection has been applied. This reconstructed mass is obtained by forcing the visible mass to be the Z boson mass and requiring the energy-momentum conservation at the given centre-of-mass energy as described in Reference [17]. After this kinematical constraint has been applied, the missing mass resolution is 3.5 GeV for a 95 GeV Higgs boson mass hypothesis.

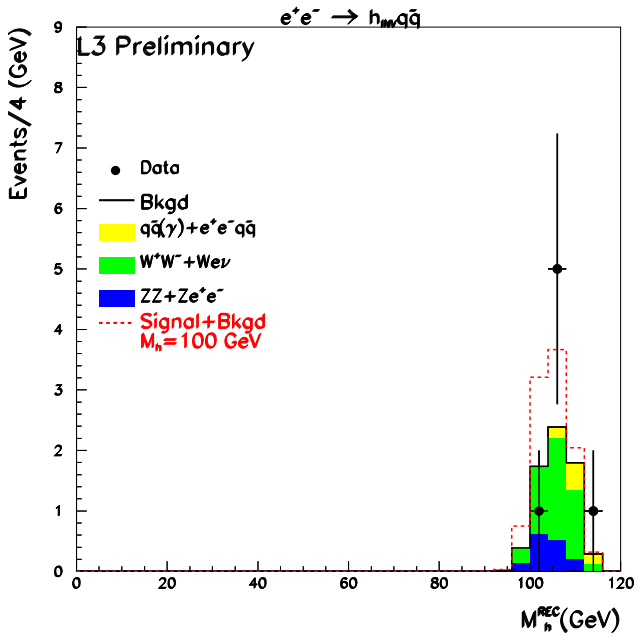

Figure 2: The distribution of the reconstructed Higgs boson mass after the heavy Higgs boson selection. The dots represent the data and the black, the dark and light shaded areas represent the $\mathrm{Z}/\gamma^*\mathrm{Z}/\gamma^* + \mathrm{Ze^+e^-}$, $\mathrm{W^+W^-} + W^{\pm}e^{\mp}\nu_e$, and $\mathrm{q\bar{q}}(\gamma) + \gamma\gamma \rightarrow \mathrm{e^+e^-q\bar{q}}$ contributions to the total background, respectively. The solid histogram represents the total background whilst the dashed histogram represents a 100 GeV Higgs boson signal added upon the total background.

3.3 Light Higgs boson selection

Complementary to the heavy Higgs boson selection, we demand events with a Z boson velocity larger than 0.4, with a visible mass larger than 60 GeV and less than 100 GeV, and we apply the same upper cut of 10 GeV on the visible energy in a cone of 30% around the beam axis.

The window applied on the visible energy, requiring it to be between 50% and 65% of the centre-of-mass energy rejects, $Z/\gamma^*Z/\gamma^*$, $W^{\pm}e^{\mp}\nu_e$ and $q\bar{q}(\gamma) + \gamma\gamma \rightarrow e^+e^-q\bar{q}$ events.

We demand to have a moderate sum of the minimum jet-jet angles when the events are forced into 3 jets, $\Theta_{123} < 303.7°$. This cut essentially reduces the $q\bar{q}(\gamma)$ and the two-photon background processes contamination.

A further rejection of the $q\bar{q}(\gamma)$ and Ze^+e^- backgrounds is obtained by tightening the cut on the cosine of the polar angle of the jets and missing momentum vector. We require its maximum value to be less than 0.98.

We cut on the acoplanarity to be less than 171.9°. This reduces the $q\bar{q}(\gamma)$, $\gamma\gamma \rightarrow e^+e^-q\bar{q}$ and Ze^+e^- background contaminations.

We apply a cut on the transverse momentum imbalance, demanding that it is between 20% and 60% of the visible energy. This cut removes most of the remaining $q\bar{q}(\gamma)$, $\gamma\gamma \rightarrow e^+e^-q\bar{q}$ and Ze^+e^- background while keeping most of the light Higgs boson signal.

Three-jet events are rejected by requiring that the DURHAM $y_{\rm cut}$ triggering between the three-jet and two-jet topologies, denoted y_{23}, is smaller than 0.03. This cut rejects events from W pair production.

The maximum energy accepted in the missing momentum vector isolation cone is set to 5 GeV.

Figure 3 displays the comparison between the data and the Monte Carlo expectations after the light Higgs boson selection on the reconstructed Higgs boson mass distributions.

$hq\bar{q}$ analysis		
	Heavy Higgs sel.	Light Higgs sel.
N_{data}	7	7
N_{bg}	6.6	10.9
$\gamma\gamma \rightarrow e^+e^-q\bar{q}$	0.	0.
$\gamma^*/Z \rightarrow q\bar{q}(\gamma)$	0.8	0.1
$W^+W^- - e^{\pm}\nu_e q\bar{q}'$	1.5	7.0
$\gamma^*/Z, \gamma^*/Z$	1.5	1.6
$e^{\pm}\nu_e q\bar{q}'$	2.8	2.2
Ze^+e^-	0.	0.

Table 2: The number of observed events, N_{data}, compared to the number of expected events from Standard Model processes, N_{bg}, after the heavy and ligth Higgs boson selection cuts.

3.4 Summary of the preliminary results in the hadronic channel

After the light Higgs boson selection, the remaining background is almost exclusively due to W pair and single W production. For the heavy Higgs boson selection, the $Z/\gamma^*Z/\gamma^*$ production is the dominant background. After the two final hadronic selections, the $q\bar{q}(\gamma)$ background is effectively eliminated.

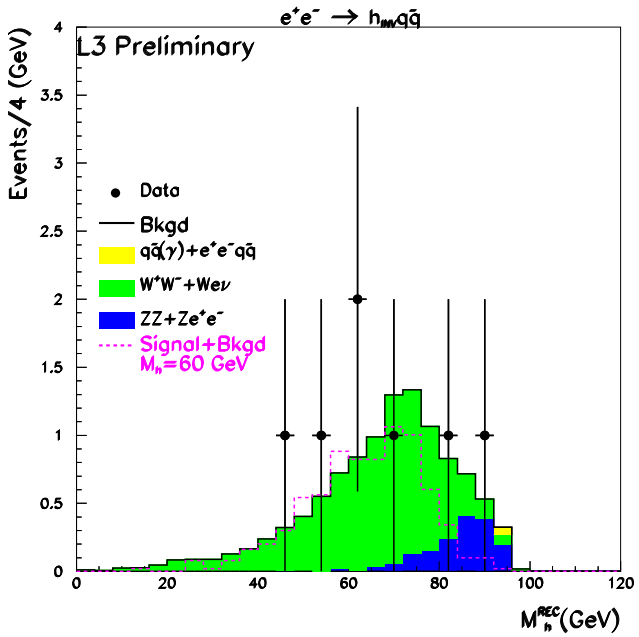

Figure 3: The distribution of the reconstructed Higgs boson mass after the light Higgs boson selection. The dots represent the data and the black, the dark and light shaded areas represent the $\mathrm{Z}/\gamma^*\mathrm{Z}/\gamma^* + \mathrm{Ze^+e^-}$, $\mathrm{W^+W^-} + W^{\pm}e^{\mp}\nu_e$, and $\mathrm{q\bar{q}}(\gamma) + \gamma\gamma \rightarrow \mathrm{e^+e^-q\bar{q}}$ contributions to the total background, respectively. The solid histogram represents the total background whilst the dashed histogram represents a 60 GeV Higgs boson signal added upon the total background.

Table 3 shows the signal selection efficiencies as a function of the Higgs boson mass, they are typically around 20% and 30% for the light and heavy Higgs boson selection, respectively.

Higgs signal efficiencies (%)		
M_h (GeV)	Heavy Higgs sel.	Light Higgs sel.
60	1.10±0.21	19.33±0.05
70	0.95±0.23	19.95±0.04
80	2.10±0.15	17.94±0.05
90	4.77±0.10	9.35±0.07
100	22.04±0.04	1.85± 0.16
110	41.38±0.03	0.

Table 3: Higgs signal efficiencies as a function of the Higgs boson mass after the heavy and the light Higgs boson selection cuts. The quoted uncertainties are statistical.

4 Search in the leptonic channel

This analysis is based on the presence of two energetic and well separated leptons ($\ell = e, \mu$) with high missing energy. The mass of the lepton pair is required to be close to the Z boson mass. The main backgrounds with low multiplicity final states are events from the two-photon interaction and fermion-pair production. These are rejected by applying a cut on the dilepton invariant mass and on the visible energy. The $W^+W^- \to \ell^+\nu\ell^-\bar{\nu}$ is the main background to this channel while the $Z/\gamma^*Z/\gamma^* \to \ell^+\ell^-\nu\bar{\nu}$ is an irreducible background but with a relatively low cross section. This analysis is almost independent of the Higgs boson mass in the range 60 GeV to 120 GeV. The event selection is designed to be almost independent of the Higgs boson mass in the investigated range.

4.1 Event Selection

Two or three charged tracks and less than 15 calorimetric clusters are required to reject high multiplicity events. The energy in the hadronic calorimeter has to be less than 10 GeV for the electron channel. To reject Bhabha events, the energy of the most energetic lepton is required to be less than $0.45\sqrt{s}$, and the cosine of the acoplanarity has to be greater than -0.999 to remove a large part of radiative lepton pair production. We also require a visible energy between 60 GeV and 130 GeV with an energy in the luminosity detectors less than 20 GeV and in small angle calorimeter ($4^\circ < \theta < 9^\circ$) less than 6 GeV. To remove the cosmic ray background, at least one scintillator in time with the beam crossing is required. Table 4 shows the comparison between data and expected Standard Model background at this level of cuts so called preselection. The discrepancy is due to the use of Monte Carlo samples generated at $\sqrt{s} = 202$ GeV $e^+e^- \to e^+e^-(\gamma)$, $e^+e^- \to \mu^+\mu^-(\gamma)$, and $e^+e^- \to \tau^+\tau^-(\gamma)$ processes removed by the following cuts described below.

Two additional selection criteria are defined:

- $|\cos\theta_{\rm MIS}| < 0.95$ to reject the radiative return to the Z peak events where $\theta_{\rm MIS}$ is the polar angle of the missing momentum. A cut is placed on the cosine of the acoplanarity which has to be greater than -0.999 to remove a large part of radiative lepton pair production. Table 4 shows the agreement between data and expected Standard Model background after this intermediate selection is applied.

- $\cos\theta^* < 0.95$ to remove $e^+e^- \to \tau^+\tau^-(\gamma)$ events where θ^* is the angle in the Z rest frame between the most energetic lepton and the direction of the Z momentum. If leptons are not coming from Z boson but from two different particles, the distribution of $\cos\theta^*$ is not flat and for example, is peaked at high value for $\tau^+\tau^-$ events. The velocity, β, of the dilepton system has to be lower than 0.65 to reduce a large fraction of two-photon interactions. As the invariant mass, $M_{\ell\ell}$, must be compatible with the Z mass, we require 80 GeV $< M_{\ell\ell} <$ 100 GeV. This last criterion reduces a large fraction of background events. Table 4 gives the number of observed and expected events after all cuts applied so called final selection..

4.2 Summary of preliminary results in leptonic channel

The selection efficiencies are approximately 48% for electron channel and 30% for muon channel. The resolution on the missing mass is 1 GeV in the electron channel and 5 GeV in the muon

e^+e^- analysis			
	Preselection	Intermediate	Final
$e^+e^- \to e^+e^-(\gamma)$	8.6	0	0
$e^+e^- \to \tau^+\tau^-(\gamma)$	5.6	0	0
$e^+e^- \to e^+e^-\tau^+\tau^-$	0.2	0	0
$e^+e^- \to e^+e^-e^+e^-$	0.6	0.2	0
$e^+e^- \to Z/\gamma^*Z/\gamma^*$	0.6	0.5	0.3
$e^+e^- \to W^+W^-$	7.1	6.7	1.5
$e^+e^- \to Ze^+e^-$	0.8	0.7	0.1
N_{bg}	23.5	8.6	1.9
N_{data}	35	10	4

$\mu^+\mu^-$ analysis			
	Preselection	Intermediate	Final
$e^+e^- \to e^+e^-\tau^+\tau^-$	0.1	0.1	0
$e^+e^- \to e^+e^-\mu^+\mu^-$	11.9	5.4	0
$e^+e^- \to \mu^+\mu^-(\gamma)$	15.4	0.7	0.1
$e^+e^- \to \tau^+\tau^-(\gamma)$	2.5	0.6	0
$e^+e^- \to Z/\gamma^*Z/\gamma^*$	0.6	0.5	0.3
$e^+e^- \to W^+W^-$	5.0	4.8	1.1
N_{bg}	35.6	12.2	1.5
N_{data}	42	16	2

Table 4: Number of observed events, N_{data}, compared to the number of expected events,N_{bg}, from Sandard Model processes after preselection cuts, after the intermediate selection criteria applied on θ_{MIS} and on the acoplanarity and after the final selection criteria.

channel for a Higgs boson mass of 90 GeV. In electron channel, 4 events are observed for 1.9 ± 0.12 events expected from the Standard Model. In muon channel, 2 events are selected for 1.5 ± 0.14 expected events. Figure 4 displays the Higgs boson mass distributions for the search in the leptonic channel.

5 Combination of results and limits

Comparing distributions of the observed and the expected number of events, we set a limit on the rate invisibly decaying Higgs boson production. In order to derive this limit, a frequentistic confidence level calculation is done according to the method proposed in [14]. The reconstructed Higgs boson mass distributions (see for example Figures 5, 6) are used in the calculation of the confidence level. For this computation, we use the Standard Model Higgs boson cross section as given by the HZHA generator [15].

The $e^+e^- \to hZ$ production cross section and the branching ratio into visible and invisible final states of a non-minimal Higgs boson h are model dependent. Thus we set an experimental upper limit on the rate of invisible Higgs boson final states, relative to the Standard Model Higgs boson rate, $R_{inv} = BR(h \to \text{invisible particles}) \times \sigma(e^+e^- \to hZ)/\sigma(e^+e^- \to H_{SM}Z)$, as a function of the Higgs boson mass. This limit which can be used to bound the parameter space

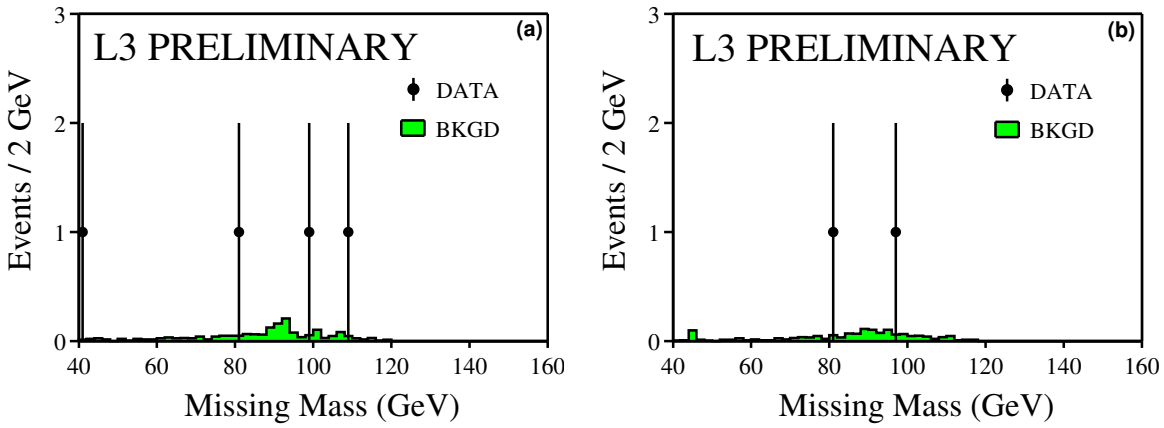

Figure 4: The Higgs boson mass distributions in the electron channel (a) and in the muon channel (b). The dots are data and the solid histograms are Monte Carlo.

of the different models predicting invisible Higgs boson decays, is shown in Figure 7 for Higgs boson masses above 50 GeV. The shaded region of this figure is excluded at least at the 95% confidence level.

Combining these inputs with those of lower energies ($\sqrt{s} = 91, 161, 172$ GeV) [17], ($\sqrt{s} = 183 - 189$ GeV) [18], ($\sqrt{s} = 192 - 202$ GeV) [19], a preliminary lower observed limit is set on the mass of an invisibly decaying Higgs boson at the 95% confidence level

$$M_h > 100.0 \text{ GeV}$$

assuming that the Higgs boson production cross section $\sigma(e^+e^- \rightarrow hZ)$ is the same as for the Standard Model Higgs boson and the Higgs boson branching ratio into invisible particles, BR(h $\rightarrow$ invisible particles), is 100%. Under the same assumptions, the expected lower limit is 104.3 GeV.

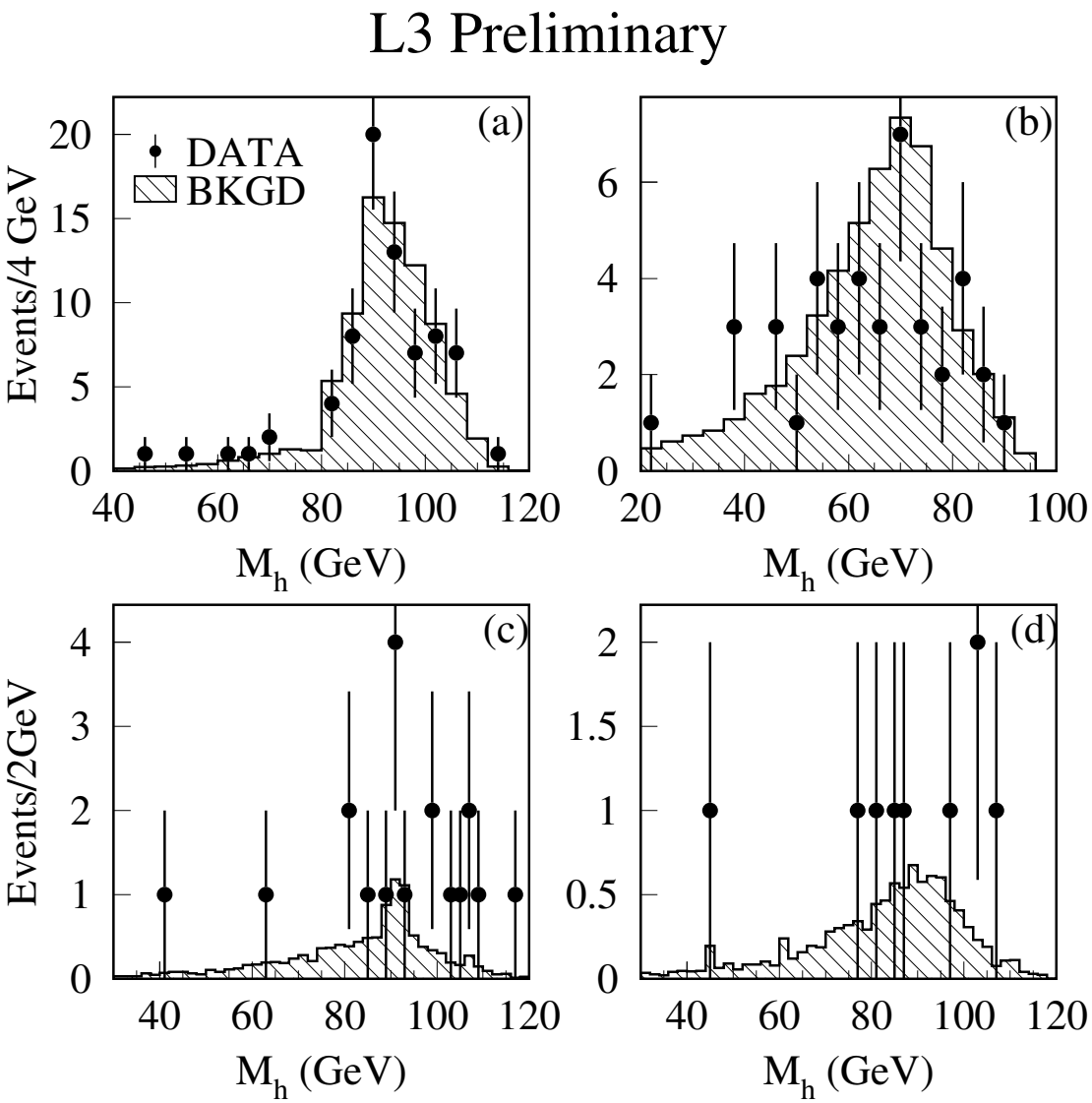

Figure 5: The Higgs boson mass distributions in the hadronic channel: heavy (a) and light (b) Higgs boson selection, in the electron channel (c) and in the muon channel (d). All analyses on invisible Higgs boson searches performed in L3 from a center-of-mass energy of 183 GeV up to 209 GeV.

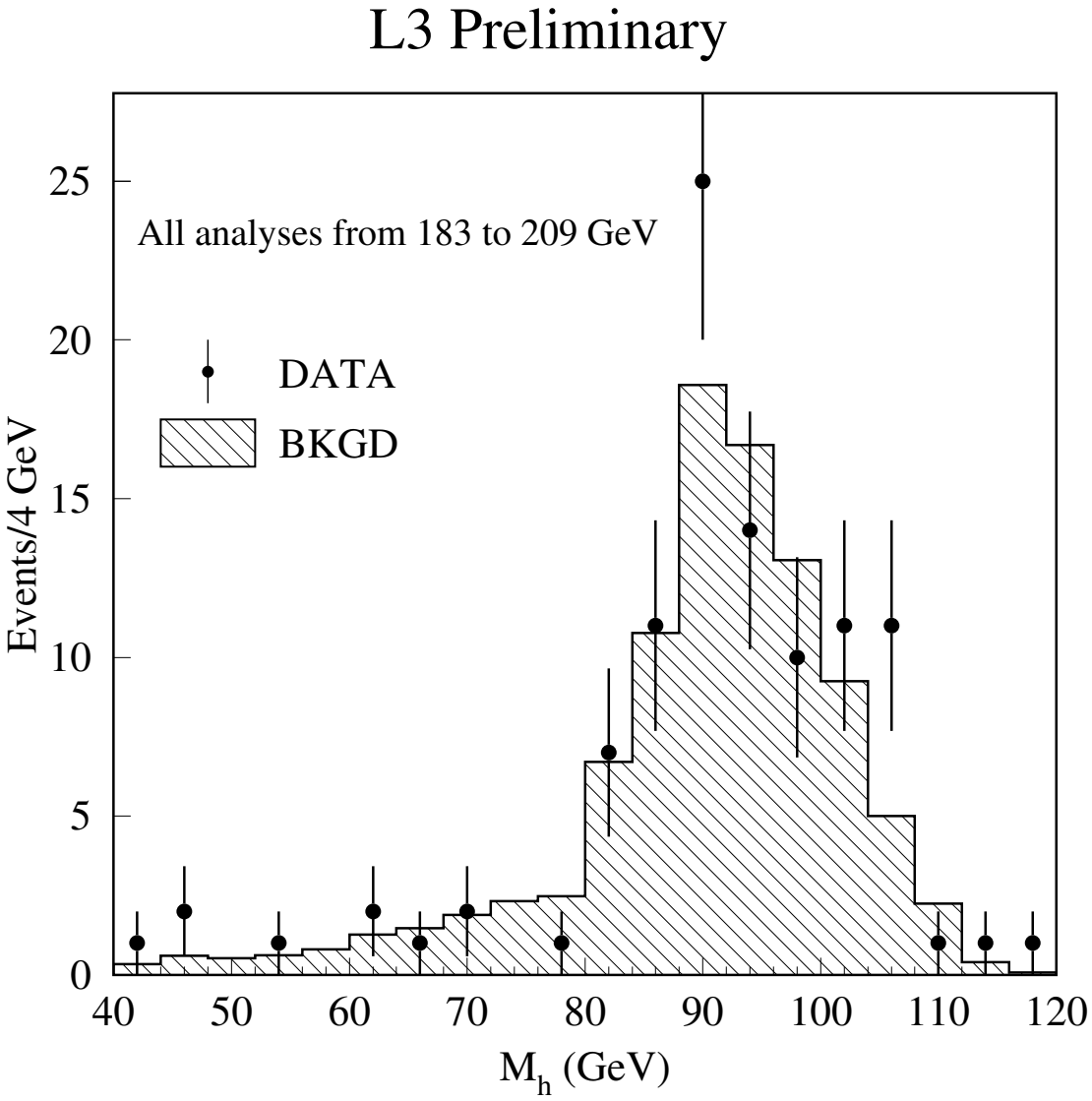

Figure 6: The Higgs boson mass combined distributions from all the searches on invisible Higgs boson performed in L3 from a center-of-mass energy of 183 GeV up to 209 GeV.

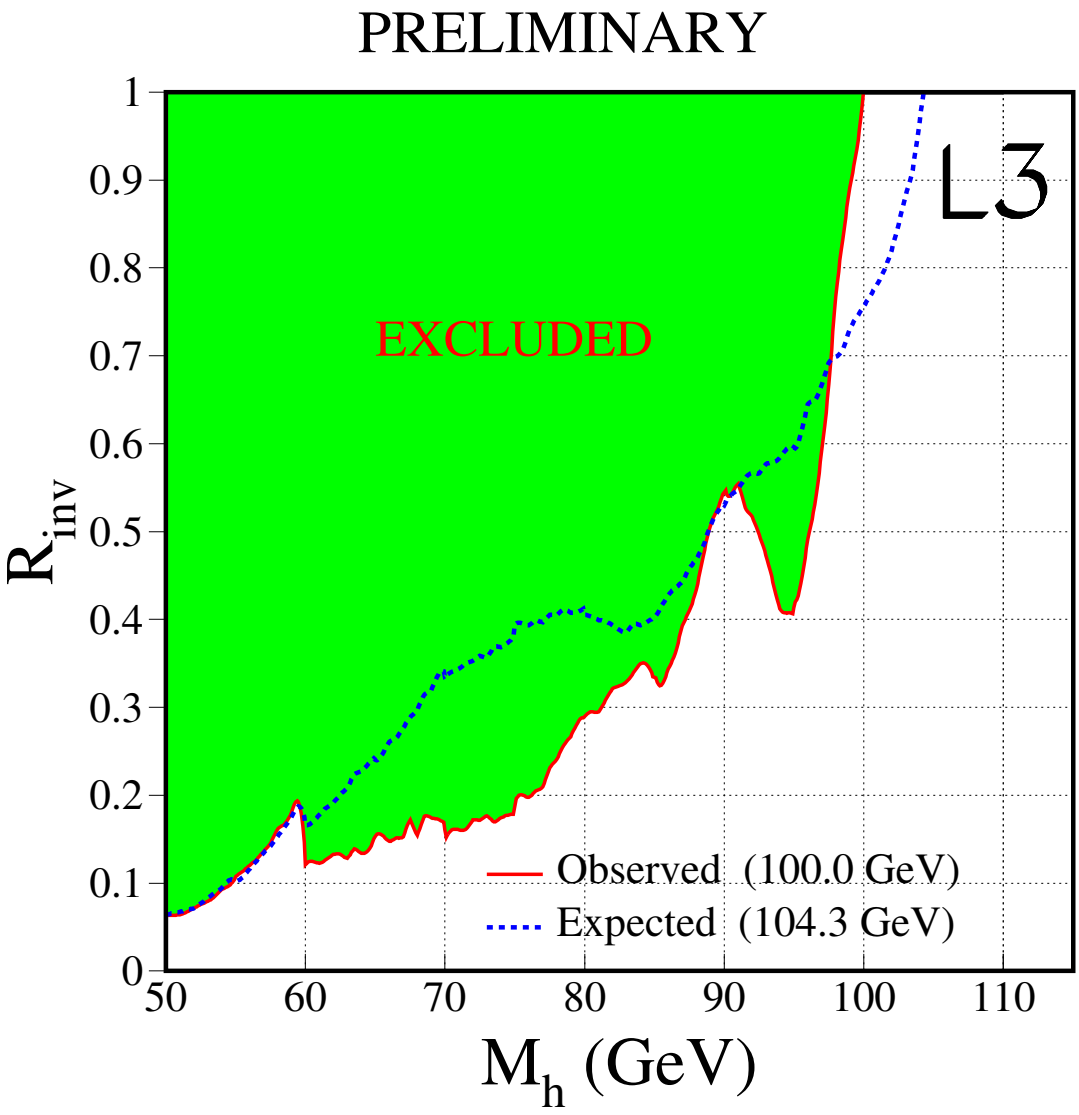

Figure 7: The upper limit on the rate of invisible Higgs boson decays, relative to the Standard Model Higgs boson production rate. These limits are based on the combination of all the analysis on invisible Higgs boson searches performed in L3 up to a center-of-mass energy of 209 GeV. For $R_{inv} = BR(h \to inv.) \times \sigma(e^+e^- \to hZ)/\sigma(e^+e^- \to H_{SM}Z) = 1$, the expected limit is $M_h > 104.3$ GeV and the observed one is $M_h > 100.0$ GeV, both at the 95% confidence level.

Acknowlegdements

We wish to express our gratitude to the CERN Accelerator Divisions for the good performance of the LEP machine. We acknowlegde the efforts of the engineers and technicians who have participated in the construction and maintenance of this experiment.

References

[1] K. Griest and H.E. Haber, Phys. Rev. **D 37** (1998) 719; A. Djouadi, P. Janot, J. Kalinowski and P.M. Zerwas, Phys. Lett. **B 376** (1996) 220.

[2] L3 Collaboration, B. Adeva et al., Nucl. Instr. Meth. **A 289** (1990) 35; J.A. Bakken et al., Nucl. Instr. Meth. **A 275** (1989) 81; O. Adriani et al., Nucl. Instr. Meth. **A 302** (1991) 53; B. Adeva et al., Nucl. Instr. Meth. **A 323** (1992) 109; K. Deiters et al., Nucl. Instr. Meth. **A 323** (1992) 162; M. Chemarin et al., Nucl. Instr. Meth. **A 349** (1994) 345; B. Acciarri et al., Nucl. Instr. Meth. **A 351** (1994) 300; G. Basti et al., Nucl. Instr. Meth. **A 374** (1996) 293; A. Adam et al., Nucl. Instr. Meth. **A 383** (1996) 342.

[3] L3 Collaboration, M. Acciarri et al., Phys. Lett. **B 418** (1997) 389.

ALEPH Collaboration, R. Barate et al., Phys. Lett., **B 466** 1999 50.

DELPHI Collaboration, P. Abreu et al., Phys. Lett. **B 459** (1999) 367.

OPAL Collaboration, G. Abbiendi et al., Eur. Phys. J. **C 7** (1999) 407.

[4] T. Sjöstrand, CERN-TH/7112/93 (1993), revised August 1995; T. Sjöstrand, Comp. Phys. **Comm. 82** (1994) 74.

[5] M. Skrzypek et al., Comp. Phys. **Comm. 94** (1996) 216; M. Skrzypek et al., Phys. Lett. **B 372** (1996) 289.

[6] S. Jadach, B.F.L. Ward, Z. Wąs, Comp. Phys. **Comm. 79** (1994) 503.

[7] R. Engel, Z.Phys. **C 66** (1995) 203; R. Engel, J. Ranft and S. Roesler, Phys.Rev. **D 52** (1995) 1459.

[8] F.A. Berends, P.H. Daverfeldt, R. Kleiss, Nucl. Phys. **B 253** (1985) 441.

[9] S. Jadach, W. Placzeck, B.F.L. Ward, Phys. Rev. **D 40** (1989) 3582; Comp. Phys. Comm. **70** (1992) 305; Phys. Lett. **B 390** (1997) 298.

[10] R. Kleiss and R. Pittau, Comp.Phys. **Comm. 83** (1994) 14.

[11] R. Brun et al., preprint CERN DD/EE/84-1 (Revised 1987).

[12] H. Fesefeldt, RWTH Aachen Report PITHA 85/02 (1985).

[13] Y.L. Dokshitzer, Contrib. to the Workshop on Jets at LEP and HERA, Durham (1990); N.Brown, W.J. Stirling, Rurherford Preprint RAL-91-049; S. Catani et al., Phys. Lett. B 269 (1991) 432;
S. Bethke et al., Nucl. Phys. **B 370** (1992) 310.

[14] A. Favara and M. Pieri, "Confidence Level Estimation and Analysis Optimization", HEP-EX/9706016 (1997).

[15] P. Janot, "The HZHA generator", in "Physics at LEP2", Eds. G. Altarelli, T. Sjöstrand and F. Zwirner, CERN 96-01 (1996) Vol.2, 309.

[16] M. Acciarri *et al.*, L3 Collaboration, Phys. Lett. **B 431**, (1998) 437-450.

[17] M. Acciarri *et al.*, L3 Collaboration, Phys. Lett. **B 418** (1998) 389-398.

[18] M. Acciarri *et al.*, L3 Collaboration, CERN-EP-2000-047, (Phys. Lett. **B** accept.).

[19] P. Lebrun, L. Lugnier and S. Muanza, L3 note 2508.